Nondeterministic multi-scale failure analysis in a woven composite fabric with a circular hole

Ahmad Kamal, Department of Mechanical and Energy Engineering, Shahid Beheshti University, Tehran, Iran,

Sayed Hossein Dibajian*, Department of Mechanical and Energy Engineering, Shahid Beheshti University, Tehran, Iran, h_dibajian@sbu.ac.ir

Abstract

Uncertainties during the manufacturing process of composite parts cause the stress field to be uncertain, and there is a range of stress concentration coefficients instead of an exact number for the stress concentration. In this study, the stress field and failure of woven composite fabric with an open hole were investigated using multiscale statistical analysis. Using analytical relations and numerical methods, the mechanical properties of a woven composite fabric were homogenized by multiscale analysis. The results of the finite element analysis of the macroscale structure were localized at the meso-scale. The various failure criteria of the composite materials around the hole were investigated using finite element analysis. Thus, the stress concentration coefficient of the composite woven fabric was obtained using these two failure criteria. A comparison of the experimental tests and multi-scale simulation results shows that the multi-scale analysis method is reliable, and confirms that the geometric uncertainties of a hole in a woven composite plate lead to different stress values around the hole in different situations. The values of the stress coefficients in the fibers varies between 1.97 and 3.09. This parameter is between 2.44 and 2.80 in the matrix. It has also been shown that from a nondeterministic point of view, the stress concentration coefficient can be estimated using a multi-scale method.

Keyword: multi-scale analysis, nondeterministic concentration coefficient, finite element method, woven composite fabric, circular hole

Highlights:

- A multi-scale analysis method to investigate woven composite fabric characteristics
- Comparison of different methods of homogenization of composite properties
- Non-deterministic study of stress concentration coefficient in composite with a hole

1- Introduction

In almost all engineering applications, parts have various geometric discontinuities that affect their strength. These discontinuities include holes used to connect components or changes in dimensions. In addition, especially in the case of composite materials, during use or production, damages are inevitable, and these damages are the source of reducing the strength and life duration of the parts. Therefore, investigating the effect of a hole and the effect of its dimensions on the strength of parts is one of the issues raised in mechanical engineering, which is one of the basic challenges regarding composite materials.

The stress concentration in holes in composite plates depends on various parameters such as fiber arrangement, the type of fiber and matrix as well as the loading, and based on this, many studies have been done with different approaches [1]. Experimental tests have shown that the tensile strength of laminated composites with holes depends on the size and shape of the hole, and this fact cannot be evaluated using the classical stress concentration coefficient. One of the criteria for the strength of composite materials with holes is the equations provided by Whitney and Nuismer [2]. They have proposed two criteria for the fracture strength of laminated composites with cracks or holes, which are in good agreement with experimental results in the case of uniaxial tension and are widely used in design due to their simplicity.

In the studies conducted by Kim et al. [3] the effect of hole size and specimen width on the fracture behavior of woven composite plates has been investigated experimentally. Based on these experiments, a relation for the characteristic length of composite with a hole is proposed, which depends on the specimen width and the hole diameter. Experimental studies on the effect of holes have been followed up with different methods. One of the conventional methods is to use image processing of the specimen under tension to determine the strain. With the method mentioned in reference [4] in a composite with woven fabric, the strain concentration around the circular or oval hole and in reference [5] the stress concentration around the circular hole has been investigated.

Numerous criteria were adapted to fit the experimental results to predict the strength of brittle materials due to the presence of stress concentration in [6]. By conducting tests and studying different criteria, the authors in this reference have concluded that one and two-parameter criteria are not suitable for evaluating the strength and size effect of brittle materials such as composite materials. So they proposed a new fracture criterion with three material parameters based on the finite fracture mechanics. Camanho et al examined the use of a continuum damage model to predict strength and size effects in carbon-epoxy laminated composites [7]. In this article, the proposed method has been compared with three conventional methods of estimating the size effect, including point stress, linear fracture mechanics, and inherent flaw model. The results indicate that the continuum damage model is the most accurate technique to predict size effects in composites. In the most of basic criteria, the fracture characteristics (strength and toughness) are evaluated separately. In the studies conducted by Martin et al. [8], a coupled measure of strength and energy is proposed for the prediction of the open hole tensile strength of a composite plate. According to this model, as the size of the hole increases, the strength of the specimen decreases. This model, which is an extension of the point stress criterion, relates the fracture characteristics and geometry (hole radius and part width).

An extensive experimental program has been performed to investigate the effect of scaling on the tensile strength of notched composites in the studies of Green et al [9]. In these studies, by keeping constant the ratio of the hole diameter to the length and width of the test sample and changing its size, the effect of scaling the specimen in the tensile test has been investigated. In most cases, as size increases, strength decreases. In addition, three distinct failure mechanisms have been observed. Despite the differences in failure stress and mechanism, similar sub-critical damage mechanisms were seen for all specimen sizes.

Proposing models based on the combination of toughness and stress criteria have been also done by other researchers. Camanho et al., based on finite fracture mechanics, proposed a model for predicting the open-hole tensile strength of composite laminates. In the proposed model, the ply elastic properties and the laminate unnotched strength and fracture toughness are used, and no empirical adjusting parameters are required [10]. Another example of energy-stress coupled models is also proposed in [11]. In the studies

conducted by Arteiro et al to predict the tensile and compressive behavior of thin-ply non-crimp laminated composites, point stress analysis methods, average stress and finite fracture mechanics have been evaluated, and the limited fracture mechanics method has been recognized as a better method for this purpose [12].

In the mentioned studies, the fiber direction of the composite material was not considered. Analysis of the effect of a stress raiser on the strength of a unidirectional composite in off-axis tension has been investigated in reference [13]. In this study, a coupled stress-strength model is used for this purpose. The evaluation of the effect of elliptical holes on the fracture strength of unidirectional composites has also been done in [14]. For composite materials including short glass fiber reinforced polyamide fibers, the fracture of notched specimen has been investigated in [15].

To investigate the effect of holes in composite materials, it is also important to study their microstructures. The microstructure of a composite material is effective in all behaviors and characteristics. The study of the effect of the behavior of microstructures and its relationship with the characteristic length parameter, which is used in the primary criteria, for three different types of cracks (circular holes, long cracks, and short cracks) has been done by Taylor [16]. In all cases, it was shown that the value of the characteristic length is simply related to the length parameter of the microstructure, and the constant value of the critical distance can be used to predict the effect of different features (holes, slots, and short cracks) that have very different stress concentration factors.

Although it has been a long time since Whitney and Nuismer's [2] criterion was proposed to analyze the hole effect in composite materials, it is still used as a method for analysis. In [17], a design tool based on the Whitney-Nuismer model is proposed to predict the failure strength of open-hole composite laminates subjected to in-plane tensile and compressive loads, and four different phenomenological equations were proposed to estimate the characteristic distances as a function of the geometric ratio; an average value, a linear variation, a parabolic variation and a function of the square root.

In woven composites, the effect of warp, weft, and matrix, the interaction between these components, and even the effect of the fibers forming are effective in the overall properties of the material. Furthermore, several methods have been developed to predict the behavior of composite materials based on this [18]. One of the conventional methods to consider these parameters is multi-scale analysis, which simultaneously relates the properties of composites in the micro-scale (microstructure) and macro scale. Using the finite element method for multi-scale modeling of composites has become common in recent years to predict the mechanical properties of composites [19, 20]. An example of this homogenization is provided in [21]. In this reference, a simple model which considers the two-dimensional extent of a woven fabric is developed. A micromechanical composite material model for woven fabric with nonlinear stress-strain relations is developed and implemented in ABAQUS for nonlinear finite element structural analysis. In [22], the stress of different components in a woven composite has been calculated on the micro and macro scale under in-plane loads by using the finite element method. The numerical methodology developed in this study can help aerospace designers optimize in-service loading conditions to prevent fracture in the tows and to increase the strength of aerospace structures utilizing such advanced composite systems.

Finite element simulation of various tests as an alternative to experimental tests to determine the properties of a woven composite has been done in [23] and it is found that a good agreement between material properties obtained from virtual characterization and experimental results. TexGen code is another tool used for homogenization. In [24], the fabric geometries are generated using TexGen and analyzed using Abaqus software to predict their mechanical properties. This method provides the possibility of creating a virtual laboratory for the analysis of various parameters of the structure.

There are four different approaches that are commonly used to create the matrix and the reinforcement parts [25] a) The reinforcement volume is subtracted from the part, then the reinforcement parts are combined to create the partitioned volume, (b) partitioning the spatial locations (surfaces/volumes) of the reinforcement parts from the matrix without cutting the matrix, c) using embedded element method [26] and d) meshing the part and assigning different properties to the elements. For fiber and matrix finite element analysis, there are some drawbacks in generating a suitable mesh for separate fiber and matrix

modeling in a and b approaches [27]. In this article, all four methods are investigated for a two-dimensional example and it is shown that although the embedded element method is suitable for reinforcement with high Young's modulus, this method is not suitable for reinforcement with low Young's modulus. By this analysis the fourth method, meshing the part and assigning different properties to the elements, is recognized as the best method.

Even though many studies have been done on the homogenization of the composite material's properties, attention to the random nature of the influential parameters in this homogenization has been paid less attention. Statistical finite element analysis provides the possibility to investigate the effect of these random variables [28-30]. The random parameters in microstructures of composites are more important in samples containing holes. In addition to the mechanical and geometric variables of the composite material, the hole position and shape are also added to the random parameters. The effect of hole shape on the reliability of laminated composites has been investigated in [31].

In this article, by using a multi-scale analysis method and statistical comparison of its results, the effect of holes on stress and failure of woven composite fabrics is investigated. During the multi-scale analysis in homogenization from micro to meso scale, the characteristics of its constituent yarns are obtained by using theoretical relationships of fiber properties. In the next step, according to the obtained properties and the geometric characteristics of the warp and weft, the homogenized properties of the woven composite fabric are obtained using finite element simulation of a representative volume element (RVE) in Abaqus.

The obtained homogenized properties are used to analyze the woven composite fabric at the macro scale. The displacement results of macro-scale simulation were used in localization as the boundary condition. In this localization, the stress field is analyzed statistically in the non-homogeneous material components in a small boundary of the whole material. The analysis of the various situations of the woven composite components around the hole can provide the designer with a suitable tool to check the uncertainties affecting of the stress concentration around the hole. Figure 1 shows the process diagram and input data in each step.

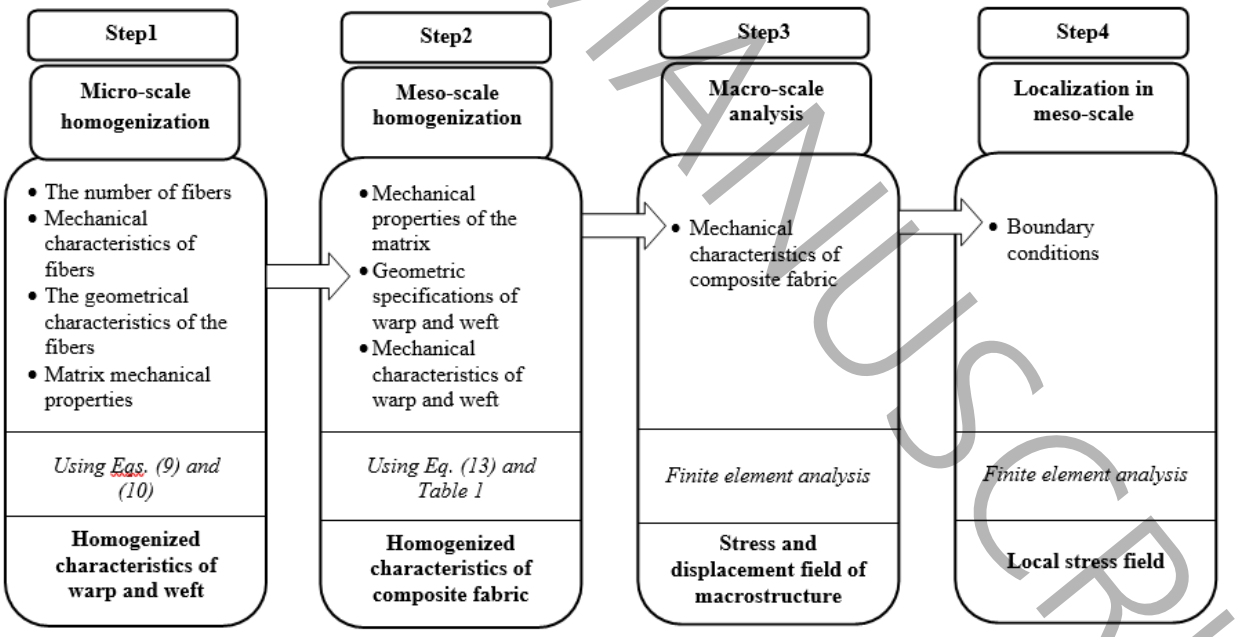

Figure 1-Process diagram and input and output data in each step

The comparison of experimental tests and simulation confirms the reliability of this multi-scale analysis method. By examining the effect of the hole size in woven composite fabric on the stresses around the hole, it is concluded that with the increase in the dimensions of the hole, the change of the maximum stress occurs at a lower rate, and therefore, the size effect decreases in holes with a larger diameter. In woven composites, in case the dimensions of the hole are not large enough compared to the yarns, uncertainties

arise due to the different positions of the warp and weft relative to the hole. Therefore, it is not possible to calculate the value of the stress concentration coefficient from a definitive point of view. So, for proper calculation of stress concentration factor, it is necessary to consider different conditions. The evaluation of the stress in different positions of the yarn relative to the hole shows that in each failure criteria of composite materials, there is a range of stress concentration coefficient values, and it is not possible to determine an explicit value for reliability.

2-Composite plate with an open-hole under tension

As mentioned, the strength of composites with open-hole has been investigated in many studies. The stress distribution around a hole in an orthotropic infinite plate is estimated by Lekhnitskii as follows[32].

$$\sigma_y(x,0)=\frac{\overline{\sigma}}{2}\left\{2+\left(\frac{R}{x}\right)^2+3\left(\frac{R}{x}\right)^4-\left[\left(K_T^{\infty}-3\right)\left(5\left(\frac{R}{x}\right)^6-7\left(\frac{R}{x}\right)^8\right)\right]\right\} \quad (1)$$

In this equation, x is the distance from the center of the hole, R is hole radius and $\overline{\sigma}$ is the applied stress. K_T^{∞} is the orthotropic stress concentration coefficient that is obtained for an infinite plate from Eq. (2).

$$K_T^{\infty}=1+\sqrt{\left(2\left(\sqrt{\frac{\overline{E}_{11}}{\overline{E}_{22}}}-\nu_{12}\right)+\frac{\overline{E}_{11}}{\overline{G}_{12}}\right)} \quad (2)$$

In this equation, E_{11}, E_{22} and G_{12} are orthotropic characteristic of materials. K_T^{∞} for an isotropic material is equal to 3, and for a woven composite, the values are between 2.53 and 3.48 [33].

Whitney and Nuismer introduced two different criteria called the point stress criterion and the average stress criterion. The proposed criterion is defined based on the strength of the unnotched composite and a length parameter of the discontinuity. These two criteria are as follows [2].

$$\begin{aligned}&\sigma_y(x,0)\big|_{x=R+d_0}=\sigma_0\\&\frac{1}{a}\int_R^{R+a_0}\sigma_y(x,0)dx=\sigma_0\end{aligned} \quad (3)$$

In these criteria, failure around a hole with radius of R, occurs when the stress (σ_y) at the distance d_0 (damage characteristic dimension) from the edge of the hole or the average stress at the distance a_0 from the edge of the hole is equal to the strength of the samples without hole a_0. By putting these two criteria in Eq. (1), it can obtain the following equations [33].

$$\begin{aligned}&\frac{\sigma_N^{\infty}}{\sigma_0}=2\Big/\left\{2+\xi_1^2+3\xi_1^4-\left(K_T^{\infty}-3\right)\left(5\xi_1^6-7\xi_1^8\right)\right\} && \xi_1=R/\left(R+d_0\right)\\&\frac{\sigma_N^{\infty}}{\sigma_0}=2\left(1-\xi_2\right)\Big/\left\{2-\xi_2^2-\xi_2^4+\left(K_T^{\infty}-3\right)\left(\xi_2^6-\xi_2^8\right)\right\} && \xi_2=R/\left(R+a_0\right)\end{aligned} \quad (4)$$

In these two criteria, there are two parameters d_0 and a_0, which must be calculated or tested for different shapes and dimensions of the hole.

In the equations proposed by Whitney and Nuismer, the characteristic lengths d_0 and a_0 are assumed as material properties. However in the studies conducted by Kim et al., it was found that these parameters

depend on the hole diameter [3]. In the improved criterion proposed for the point stress criterion, the characteristic length is obtained from the following equation.

$$d_0 = k^{-1}\left(2R/W\right)^m \tag{5}$$

In this equation, *k* is the notch sensitivity factor concerning *2R* the hole diameter, *W* the part width, and *m* is an exponential parameter. It is suggested to use the following equation for the relationship between the characteristic length and the final strength of the fabric, where *A* and *B* are two material constants and are obtained from experimental tests.

$$\left(\sigma_N/\sigma_0\right)_{EXP} = Ad_0 + B \tag{6}$$

Simultaneous consideration of the effects of strength and toughness was another development in the study of the hole size effect in the composite. The tensile strength proposed by Martin et al. [8], which was coupled considering the strength and toughness, is proposed as follows.

$$\frac{\sigma^*}{\sigma^C} = \sqrt{\frac{L^C}{R}}\frac{1}{\sqrt{A\left(a^*\right)}} \tag{7}$$

In this equation, σ^* is the critical stress and σ^C is the strength of the sample without cracks. L^C is the Irwin characteristic fracture length of the material and R is the radius of the hole and $A\left(a^*\right)$ is a dimensionless coefficient.

In evaluating the failure of composite materials, the criteria proposed by Chamis are used. Chamis criteria for composite material failure are as Eq. (8) [34].

$$\begin{aligned}
\left(\sigma_1^T\right)_{ult} &\approx V_f S_{fT}\\
\left(\sigma_1^C\right)_{ult} &\approx V_f S_{fC}\\
\left(\sigma_1^C\right)_{ult} &\approx 10\left(\tau_{12}\right)_{ult} + 2.5S_{mT}\\
\left(\sigma_1^C\right)_{ult} &\approx \frac{G_m}{1 - V_f\left(1 - \frac{G_m}{G_{12f}}\right)}\\
\left(\sigma_2^T\right)_{ult} &\approx \left(1 - \left(\sqrt{V_f} - V_f\right)\left(1 - \frac{E_m}{E_{22f}}\right)\right)S_{mT}\\
\left(\sigma_2^C\right)_{ult} &\approx \left(1 - \left(\sqrt{V_f} - V_f\right)\left(1 - \frac{E_m}{E_{22f}}\right)\right)S_{mC}\\
\left(\tau_{12}\right)_{ult} &\approx \left(1 - \left(\sqrt{V_f} - V_f\right)\left(1 - \frac{G_m}{G_{12f}}\right)\right)S_{mS}\\
\left(\tau_{13}\right)_{ult} &\approx \left(\tau_{12}\right)_{ult}
\end{aligned} \tag{8}$$

$$(\tau_{23})_{ult} \approx \left(\frac{1-\sqrt{V_f}\left(1-\frac{G_m}{G_{23f}}\right)}{1-V_f\left(1-\frac{G_m}{G_{23f}}\right)} \right) S_{mS}$$

In these equations, V_f is the volume fraction of fiber, E_m is the matrix modulus, E_{22m} is transverse Young's modulus of the fiber, G_m is the matrix shear modulus, G_{12f} and G_{23f} are fiber shear moduli, S_{fC} and S_{fT} are the tensile and compression strength of fibers, respectively. Also, S_{mT}, S_{mC} and S_{mS} demonstrate the tensile, compression and shear strength of matrix, respectively.

3-Multi-scale analysis

There are two basic approaches to modeling composites: the macromechanical approach and the micromechanical approach. The macromechanical approach involves constructing models strictly at the macro scale wherein the composite is viewed as an anisotropic material, and the details of the underlying arrangement of the constituent materials are ignored. In contrast, the micromechanical approach to modeling composites explicitly considers the constituent materials and how they are arranged to form the composite. The goal of micromechanics is to predict the effective behavior of a heterogeneous material based on the behavior of the constituent materials and their geometric arrangement. By determining a composite's effective behavior via micromechanics, it can then be treated as a material in higher scale analyses (similar to the macromechanical approach). Multiscale modeling of composites refers to simulating their behavior through multiple time and/or length scales [35].

Traditionally, one traverses these scales via homogenization and localization techniques, respectively, a homogenization technique provides the properties or response of a 'structure' given the properties or response of the structure's 'constituents' [35].

In this study, homogenization and localization were performed in a noncoupled manner. In the homogenization part, the elastic properties of the material were determined based on the microscale structure. Homogenization is performed in two steps: from micro to meso and from meso to macro.
In the localization part, boundary conditions were applied and analyzed in the mesoscale model after analyzing the macroscopic model. The stress concentration coefficients were then calculated based on mesoscale stresses.

3-1-Homogenization

One of the methods in the homogenization of composite structures is to consider a small part of the material as a component representing the whole material. In this method, the material is considered in a representative volume element (RVE) with full details and according to the specifications defined for this part, its effective elastic properties are obtained. These effective properties are considered as the general properties of homogeneous material in the macroscopic scale. In an RVE, the stored strain energy density must be equal to the strain energy density of the equivalent homogenized element at the same strain. This concept was first used by Hill [36]. Hill determined two conditions for the RVE. This element should be structurally a sample of the entire composite material and include enough components of the material whose apparent moduli are independent of the surface tension and displacement. Therefore, the RVE should be chosen in such a way that by repeating it in different directions, the whole material is made.

In this article, homogenization is done in two steps. Characterization of warp and weft yarns is done using analytical equations as homogenization from micro-scale to meso-scale. In these equations, the properties of the warp and weft are obtained by using the properties of their constituent fibers and matrix. In the homogenization from meso scale to macro scale in woven composite, there is no exact analytical equation and homogenization is done numerically in Abaqus software.

3-1-1-Warp and weft homogenization

The warp and weft yarns used in woven fabrics are composed of parallel thin fibers, which matrix penetrates between these fibers during the production process of composite fabric. Therefore, in composite fabrics, the warp and weft yarn should be considered as unidirectional composites, with the resin as the base material and the fibers as its reinforcement. For the homogenization of unidirectional composite materials, several methods have been proposed [35]. In woven composites, the curvature radius of the fibers is on the scale of the fiber diameter. Therefore, in the microstructure analysis of the warp and weft, the ratio of fiber curvature to fiber diameter is very large. Therefore, in the microcomposite analysis, warp and weft unidirectional composites can be considered. The effective elastic stiffness and compliance matrices of a transversely isotropic material are defined by five independent engineering constants: longitudinal and transversal Young's moduli E_{11} and E_{22}, longitudinal and transversal shear moduli G_{12} and G_{23}, and major Poisson's ratio ν_{12} (Noting that direction 1 is along the fibers). The minor Poisson's ratio ν_{23} is related to E_{22} and G_{12}. The effective elastic properties are evaluated in terms of the mechanical properties of fibers and matrix. The relationship between strain and stress in a transversely isotropic material is given as follows [37]:

$$\begin{Bmatrix} \varepsilon_{11} \\ \varepsilon_{22} \\ \varepsilon_{33} \\ \varepsilon_{12} \\ \varepsilon_{13} \\ \varepsilon_{23} \end{Bmatrix} = \begin{bmatrix} 1/E_{11} & -\nu_{12}/E_{11} & -\nu_{12}/E_{11} & 0 & 0 & 0 \\ -\nu_{12}/E_{11} & 1/E_{22} & -\nu_{23}/E_{22} & 0 & 0 & 0 \\ -\nu_{12}/E_{11} & -\nu_{23}/E_{22} & 1/E_{33} & 0 & 0 & 0 \\ 0 & 0 & 0 & 1/G_{23} & 0 & 0 \\ 0 & 0 & 0 & 0 & 1/G_{12} & 0 \\ 0 & 0 & 0 & 0 & 0 & 1/G_{12} \end{bmatrix} \begin{Bmatrix} \sigma_{11} \\ \sigma_{22} \\ \sigma_{33} \\ \sigma_{12} \\ \sigma_{13} \\ \sigma_{23} \end{Bmatrix} \tag{9}$$

Among the relationships proposed for the homogenized components of unidirectional composite materials, the equations introduced by Chamis [38] are in good agreement with the experimental results and can be considered as a complete model for accurate estimation of properties [37]. Chamis equations are as Eq. (10).

$$\begin{aligned} E_{11} &= V_f E_{11f} + V_m E_m \\ E_{22} &= \frac{E_m}{1-\sqrt{V_f}\left(1-\frac{E_m}{E_{22f}}\right)} \\ G_{12} &= \frac{G_m}{1-\sqrt{V_f}\left(1-\frac{G_m}{G_{12f}}\right)} \\ G_{23} &= \frac{G_m}{1-\sqrt{V_f}\left(1-\frac{G_m}{G_{23f}}\right)} \\ \nu_{12} &= V_f \nu_{12f} + V_m \nu_m \\ \nu_{23} &= \frac{E_{22}}{2G_{23}} - 1 \end{aligned} \tag{10}$$

In these equations, V_m is the volume fraction of matrix, E_{11} is the modulus in the longitudinal direction of fibers, E_{22} is the transverse modulus of fibers, E_{11f} is the longitudinal Young's modulus of the fiber, ν_{12f} is fiber Poisson's ratio, ν_m s matrix Poisson's ratio and ν_{12} and ν_{23} are fiber Poisson's ratio.

3-1-2-Composite woven fabric

A woven composite fabric can be considered as an orthotropic material in the macro scale. The relationship between stress and strain of an orthotropic material is generally in the form of Eq. (11). In this equation, σ is the stress tensor, D is the stiffness tensor, and ε is the strain tensor. The extended form of this equation is in the form of Eq. (12) [39].

$$\sigma = D\varepsilon \tag{11}$$

$$\begin{Bmatrix} \sigma_{11} \\ \sigma_{22} \\ \sigma_{33} \\ \sigma_{12} \\ \sigma_{13} \\ \sigma_{23} \end{Bmatrix} = \begin{bmatrix} D_{1111} & D_{1122} & D_{1133} & 0 & 0 & 0 \\ D_{1122} & D_{2222} & D_{2233} & 0 & 0 & 0 \\ D_{1133} & D_{2233} & D_{3333} & 0 & 0 & 0 \\ 0 & 0 & 0 & D_{1212} & 0 & 0 \\ 0 & 0 & 0 & 0 & D_{1313} & 0 \\ 0 & 0 & 0 & 0 & 0 & D_{2323} \end{bmatrix} \begin{Bmatrix} \varepsilon_{11} \\ \varepsilon_{22} \\ \varepsilon_{33} \\ \varepsilon_{12} \\ \varepsilon_{13} \\ \varepsilon_{23} \end{Bmatrix} \tag{12}$$

The stiffness tensor in this equation includes 9 independent parameters and 9 equation are needed to specify them.

The elastic strain energy stored in this material can be obtained from Eq. (13).

$$E = \frac{1}{2}\sigma^T\varepsilon = \frac{1}{2}\varepsilon^T\varepsilon = \frac{1}{2}\begin{Bmatrix} \varepsilon_{11} \\ \varepsilon_{22} \\ \varepsilon_{33} \\ \varepsilon_{12} \\ \varepsilon_{13} \\ \varepsilon_{23} \end{Bmatrix}^T \begin{bmatrix} D_{1111} & D_{1122} & D_{1133} & 0 & 0 & 0 \\ D_{1122} & D_{2222} & D_{2233} & 0 & 0 & 0 \\ D_{1133} & D_{2233} & D_{3333} & 0 & 0 & 0 \\ 0 & 0 & 0 & D_{1212} & 0 & 0 \\ 0 & 0 & 0 & 0 & D_{1313} & 0 \\ 0 & 0 & 0 & 0 & 0 & D_{2323} \end{bmatrix} \begin{Bmatrix} \varepsilon_{11} \\ \varepsilon_{22} \\ \varepsilon_{33} \\ \varepsilon_{12} \\ \varepsilon_{13} \\ \varepsilon_{23} \end{Bmatrix} \tag{13}$$

If an RVE is under the effect of simple strain in the direction 1, the only component of the strain tensor that has a non-zero value is ε_{11} and the stored strain energy is equal to

$$E = \frac{1}{2}\varepsilon_{11}^{\ 2} D_{1111} \tag{14}$$

Therefore, if the amount of energy stored in the RVE during applying simple strain in direction 1 is known, the value of the D_{1111} of the stiffness tensor could be calculated as Eq. (15).

$$D_{1111} = \frac{2E}{\varepsilon_{11}^{\ 2}} \tag{15}$$

Similar to this method, to determine the other components of the stiffness tensor, other hypothetical strains can be applied according to Table 1, and 9 independent components of the stiffness tensor can be calculated.

Table 1-Calculation of stiffness tensor components based on strain energy and strain values

Strain vector	*Stored elastic energy*	*Stiffness tensor component*
$\varepsilon = \begin{bmatrix} \varepsilon_{11} \\ 0 \\ 0 \\ 0 \\ 0 \\ 0 \end{bmatrix}$	$E = \frac{1}{2}\varepsilon_{11}^{2} D_{1111}$	$D_{1111} = \frac{2E}{\varepsilon_{11}^{2}}$
$\varepsilon = \begin{bmatrix} 0 \\ \varepsilon_{22} \\ 0 \\ 0 \\ 0 \\ 0 \end{bmatrix}$	$E = \frac{1}{2}\varepsilon_{22}^{2} D_{2222}$	$D_{2222} = \frac{2E}{\varepsilon_{22}^{2}}$
$\varepsilon = \begin{bmatrix} 0 \\ 0 \\ \varepsilon_{33} \\ 0 \\ 0 \\ 0 \end{bmatrix}$	$E = \frac{1}{2}\varepsilon_{33}^{2} D_{3333}$	$D_{3333} = \frac{2E}{\varepsilon_{33}^{2}}$
$\varepsilon = \begin{bmatrix} \varepsilon_{11} \\ \varepsilon_{22} \\ 0 \\ 0 \\ 0 \\ 0 \end{bmatrix}$	$E = \frac{1}{2}\varepsilon_{11}^{2} D_{1111} + \frac{1}{2}\varepsilon_{22}^{2} D_{2222} + \varepsilon_{11}\varepsilon_{22} D_{1122}$	$D_{1122} = \frac{E}{\varepsilon_{11}\varepsilon_{22}} - \frac{1}{2}\left(D_{1111}\frac{\varepsilon_{11}}{\varepsilon_{22}} + D_{2222}\frac{\varepsilon_{22}}{\varepsilon_{11}} \right)$
$\varepsilon = \begin{bmatrix} \varepsilon_{11} \\ 0 \\ \varepsilon_{33} \\ 0 \\ 0 \\ 0 \end{bmatrix}$	$E = \frac{1}{2}\varepsilon_{11}^{2} D_{1111} + \frac{1}{2}\varepsilon_{33}^{2} D_{3333} + \varepsilon_{11}\varepsilon_{33} D_{1133}$	$D_{1133} = \frac{E}{\varepsilon_{11}\varepsilon_{33}} - \frac{1}{2}\left(D_{1111}\frac{\varepsilon_{11}}{\varepsilon_{33}} + D_{3333}\frac{\varepsilon_{33}}{\varepsilon_{11}} \right)$

$\varepsilon = \begin{bmatrix} 0 \\ \varepsilon_{22} \\ \varepsilon_{33} \\ 0 \\ 0 \\ 0 \end{bmatrix}$	$E = \frac{1}{2}\varepsilon_{22}^{2} D_{2222} + \frac{1}{2}\varepsilon_{33}^{2} D_{3333} + \varepsilon_{22}\varepsilon_{33} D_{2233}$	$D_{2233} = \frac{E}{\varepsilon_{22}\varepsilon_{33}} - \frac{1}{2}\left(D_{2222}\frac{\varepsilon_{22}}{\varepsilon_{33}} + D_{3333}\frac{\varepsilon_{33}}{\varepsilon_{22}} \right)$
$\varepsilon = \begin{bmatrix} 0 \\ 0 \\ 0 \\ \varepsilon_{12} \\ 0 \\ 0 \end{bmatrix}$	$E = \frac{1}{2}\varepsilon_{12}^{2} D_{1212}$	$D_{1212} = \frac{2E}{\varepsilon_{12}^{2}}$
$\varepsilon = \begin{bmatrix} 0 \\ 0 \\ 0 \\ 0 \\ \varepsilon_{13} \\ 0 \end{bmatrix}$	$E = \frac{1}{2}\varepsilon_{13}^{2} D_{1313}$	$D_{1313} = \frac{2E}{\varepsilon_{13}^{2}}$
$\varepsilon = \begin{bmatrix} 0 \\ 0 \\ 0 \\ 0 \\ 0 \\ \varepsilon_{23} \end{bmatrix}$	$E = \frac{1}{2}\varepsilon_{23}^{2} D_{2323}$	$D_{2323} = \frac{2E}{\varepsilon_{23}^{2}}$

3-1-3- Comparison of multi-scale finite element modeling methods

There are four common methods for the simulation of multi-scale finite elements of composites. In the first method, fibers and matrix are modeled separately and then they are tied to each other. In the second method, which is more common in two-dimensional analysis, the sample volume is partitioned into two parts: matrix and reinforcement (Figure 2-a). In the third method, which is studied in [26], the fibers are modeled separately and the sample volume is completely modeled as a matrix, then they are connected via the embedded tool. (Figure 2-b). In the fourth method, first, the sample volume is meshed, and then matrix and reinforcing properties are assigned to the elements (Figure 2-c).

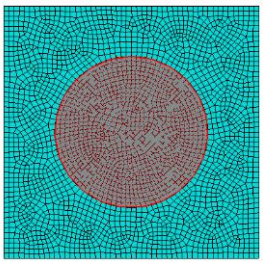
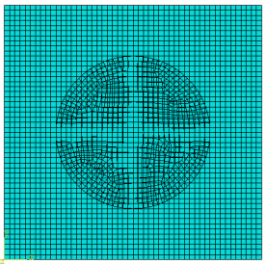
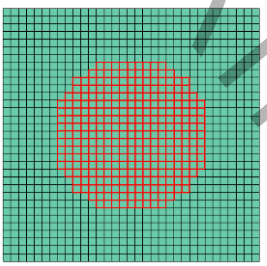

(a) (b) (c)

Figure 2- Three different method of finite element multi-scale modeling a: partitioning the part. b: embedded element. c: assigning material properties to element

Considering that the first and second methods have similar results if the element is small, only the second, third, and fourth methods have been investigated. To compare, a two-dimensional sample of 10 x 10 mm with a reinforcement of 6 mm diameter is modeled in Abaqus. It is assumed that the matrix Young's modulus is 3 GPa. The reinforcement Young's modulus is considered 200 GPa and 6 GPa in two different analyses. Symmetry boundary conditions are assumed for the lower and left boundaries, and the right boundary is moved 1 mm. In the Table 2, the results of strain energy are compared.

Table 2-comparison of calculated strain energy in different methods

	strain energy (mJ) $(E_m = 3\ Gpa, E_f = 6\ Gpa)$	strain energy (mJ) $(E_m = 3\ Gpa, E_f = 200\ Gpa)$
first and second methods	1796	2458
Third method	1959	2498
Fourth method	1797	2470

According to Table 2, the embedded element method mentioned in [26] is only suitable for certain conditions. In the analysis in the micro-scale, the difference between the properties of the reinforcement and the matrix is considerable, but in the meso-scale analysis, this difference is reduced, and therefore the embedded element method is not suitable for all cases. In three dimensions, there are some drawbacks in producing a suitable mesh in the first and second methods, and the third method has made some errors. Therefore, in this article, the fourth method is used for modeling.

3-2- Localization, stress analysis and failure assessment

Due to the multipart nature of composite materials, many failure and damage modes are caused in microstructures. Yarn failure, matrix failure, and warp and weft separation from the matrix are some of the failure modes that occur in the microstructure. That's why, the analysis of stress field in the microstructure of composite material is a crucial issue.

Localization of the composite fabric macro model in Abaqus software is done by placing and analyzing the RVE in the desired location of the macrostructure and using macro model boundary conditions to evaluate the microstructure stress field. For this purpose, first, a sub-model of the RVE is built and the built sub-model is placed in the desired location of the macrostructure. With the help of a Python script, outside elements of the sub-model are removed and the displacement boundary condition of the macro model is applied to it. The maximum stress in warp and weft elements and matrix elements is a criterion for comparing different modes in localization.

Analysis of various uncertainties that are made during the production process of composite fabrics can be a tool for the analysis of woven fabrics. The exact position of the warp and weft relative to the hole is one such uncertainty. When the dimensions of the warp and weft are not negligible compared to the dimensions of the hole, the different positions of the warp and weft relative to the hole are effective in the stress field.

The position of the hole is not fixed in relation to the warp and weft of the woven composite fabric, and the hole could have different positions. Therefore, to accurately evaluate the effect of the hole, it is necessary to consider different positions and statistically analyze the stress field. In this case, statistical parameters, such as the average maximum stress values or stress histograms, are better tools for analysis. To perform statistical analysis at different points, the micro model created in the localization step is placed in many different positions relative to the warp and weft. The more the number of repetitions of this operation, the more diverse conditions of stress are extracted in different situations.

Due to the different strengths of yarns and matrix, it is necessary to consider maximum stress in warp and weft elements and matrix elements separately. An average of 5 maximum element stresses in every

condition of yarn position relative to the hole are stored in a file by the script. By using the obtained stresses, a histogram of stress in matrix and yarns is drawn. By comparing the stress histogram in different hole diameters probability of failure in different conditions is obtained.

4- Experiments, simulations and results

To investigate the multi-scale analysis method, a tensile test of a woven composite fabric is used.

4-1- Producing test samples

4-1-1- Yarn fibers

The woven fabric used to make the samples in shown in Figure 3.

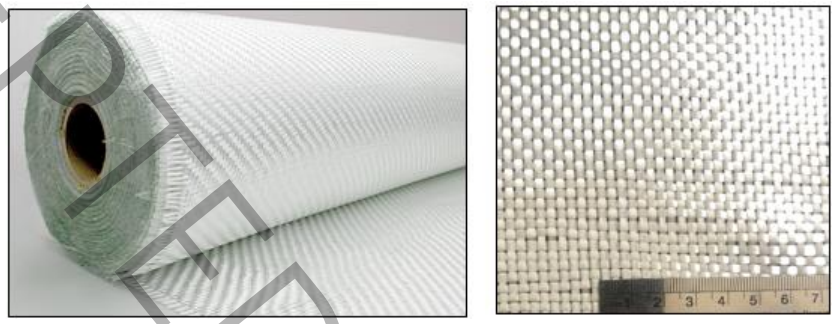

Figure 3-Woven fabric used in experiments

The glass yarns in this woven fabric are type E. The properties of the fibers used for the production of warp and weft yarns have been determined experimentally.

4-1-2- Matrix properties

The woven composite fabric matrix is made by the combination of resin epoxy EP 411 and H15 hardener. The physical, mechanical, and process characteristics of this resin based on manufacturer data are shown in Table 3. It is suggested that after the completion of the time necessary for the initial curing, the post-curing process should be applied for 3 hours under temperature conditions up to 80 ºC to improve the mechanical properties of the samples.

Table 3-EP 411 epoxy resin and H15 hardener specification

Physical/mechanical/process characteristic	Value	Test method
Viscosity at 25ºC (millipascals.seconds)	100-150	ISO 12058-1
Density at 25ºC (grams per cubic centimeter)	1.17	ISO 1675
Color	Colorless	—
Tensile strength (MPa)	50-60	ASTM D638-14
Flexural strength (MPa)	70-80	ASTM D5023-15
compressive strength (MPa)	72-75	ASTM D695-15
Heat Degradation Temperature (ºC)	90-95	—
Maximum working time per 250 grams of resin at 23ºC (hours)	150	TECAM At 65% humidity
Sufficient curing time (hours)	24	—
weight ratio of resin and hardener	10:1	—

4-1-3- Specimen manufacturing

The experimental specimens were prepared by using the vacuum molding process under the defined curing parameters. Specimen dimensions are 30 x 90 millimeters and a hole is created in the middle of the specimens using a sharp tool. In this way, 6 specimens were used in the experiments, one of which is without holes and the other 5 specimens have holes with diameters of 2, 4, 6, 8, and 10 millimeters.

The specifications of the components used in the composite woven fabric are shown in Table 4. Data in Table 4 is based on manufacturer's data or measurements.

Table 4-Specifications of the components used in the fabric

characteristic (unit)	**Value**
Warp/weft width (mm)	2
Warp/weft height (mm)	0.6
The distance between warps/wefts in fabric (mm)	0.8
The number of layers	1
The number of fibers in the warp/weft	575
The diameter of the fibers in the warp/weft (mm)	0.0072
Young's modulus of warp/weft fibers (Mpa)	79000
Poisson's ratio of warp/weft fibers	0.26
Young's modulus of resin (MPa)	2789-3500
Poisson's ratio of resin	0.35
tensile strength of fibers (MPa)	1150
compression strength of fibers (MPa)	1150
tensile strength of resin (MPa)	50
compression strength of resin (MPa)	50
shear strength of resin (MPa)	25

To determine the woven composite fabric mechanical properties, tensile tests were performed on the specimens using the ASTM D3039 (Standard test method for tensile properties of polymer matrix composite materials), and the elastic modulus of woven composite fabric was measured. This method is suitable for determining the in-plane tensile properties of composite materials reinforced with continuous fibers with high elastic modulus. In Figure 4 test specimens are shown.

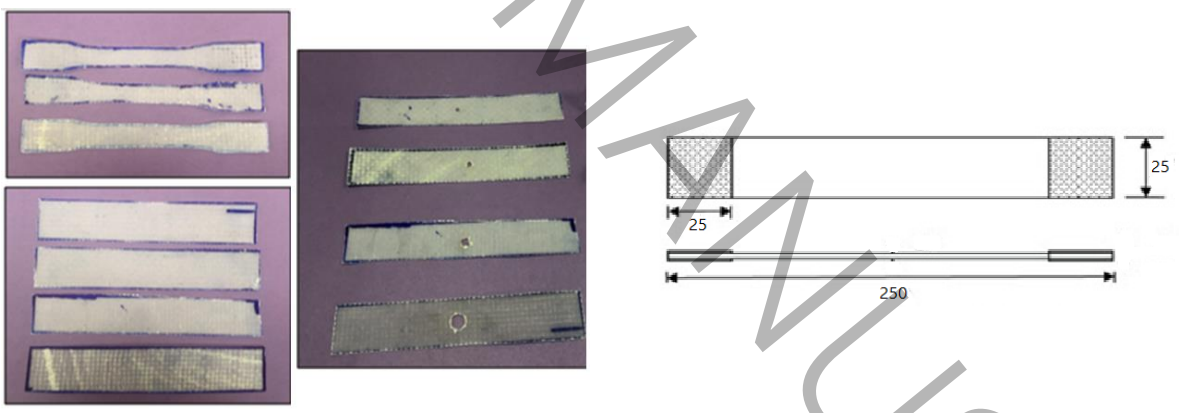

Figure 4- Composite fabrics and its standard dimensions

In Figure 5 the tensile test steps applied on woven composite fabric are shown. This test is also done on specimens with standard dimensions and both longitudinal and transverse arrangements too. To ensure reproducibility, each test was repeated twice.

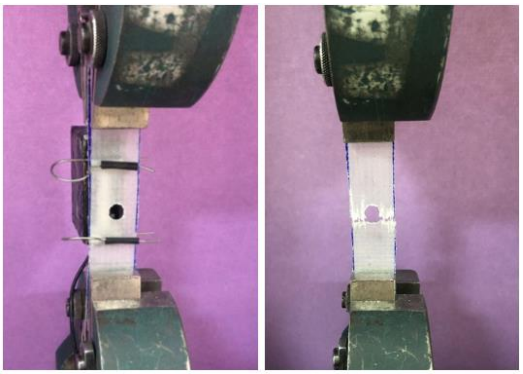

a b

Figure 5-Tensile test, a) before fracture, b) after fracture

In Figure 6 the fracture of specimens is shown.

Figure 6-Fracture of each specimen after tension

As shown in Table 5 although the specimens with 2, 4, and 6 millimeters diameter holes have fractured from the clamp area, the samples with 8 and 10 millimeters diameter holes have broken around the hole.

Table 5-Broken area for each specimen

Specimens	Broken from the clamp area	Broken around hole
Specimen with 2 mm diameter hole	✓	
Specimen with 4 mm diameter hole	✓	
Specimen with 6 mm diameter hole	✓	
Specimen with 8 mm diameter hole		✓
Specimen with 10mm diameter hole		✓

4-2-Simulation

4-2-1-Homogenization in Meso scale

To simulate the 9 experiments planned in Table 1, the RVE was simulated in Abaqus, according to the geometry and the data in Table 4.

To make the RVE, first, a cube with the RVE dimensions was regularly meshed. Then, based on the position of every element, material properties, and material orientation were assigned. The position of

warp and weft elements are specified by an Abaqus script based on race track model [40] and the properties of homogenized yarns are assigned to them. The rest of the elements contain matrix. In Figure 7 the RVE and different component of the RVE is shown.

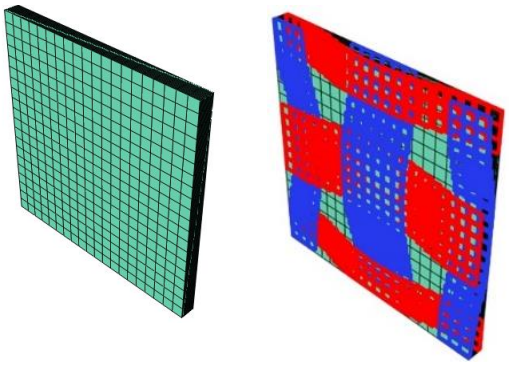

(a) (b)

Figure 7- (a) RVE used in simulation (b) Position of warp and weft elements in RVE

In the Abaqus step module, 9 steps are defined according to the boundary conditions in Table 1. According to the stored energy density calculated at each step of the simulation and taking into account the relationships in Table 1, the components of the stiffness tensor are calculated. The equivalent stiffness tensor calculated in this method is shown in Eq. (16). The verification of this equation is in section 4-3-1.

$$D=\begin{bmatrix} D_{1111} & D_{1122} & D_{1133} & 0 & 0 & 0 \\ D_{1122} & D_{2222} & D_{2233} & 0 & 0 & 0 \\ D_{1133} & D_{2233} & D_{3333} & 0 & 0 & 0 \\ 0 & 0 & 0 & D_{1212} & 0 & 0 \\ 0 & 0 & 0 & 0 & D_{1313} & 0 \\ 0 & 0 & 0 & 0 & 0 & D_{2323} \end{bmatrix}=\begin{bmatrix} 6833 & 3125 & 3104 & 0 & 0 & 0 \\ 3125 & 6770 & 3039 & 0 & 0 & 0 \\ 3104 & 3039 & 5873 & 0 & 0 & 0 \\ 0 & 0 & 0 & 1489 & 0 & 0 \\ 0 & 0 & 0 & 0 & 1518 & 0 \\ 0 & 0 & 0 & 0 & 0 & 1502 \end{bmatrix} \quad (16)$$

The calculated stiffness tensor, as a characteristic of a homogeneous material, can be used in the larger scale (macro) simulation. Therefore, by modeling the woven composite fabric as a homogenized part and using the stiffness tensor, the stress and strain fields of the fabric can be obtained. The boundary condition of the macro model was considered as displacement boundary condition similar to the tensile test. In Figure 8 stress field of simulated fabric with a 10 millimeters hole in the macro scale is shown.

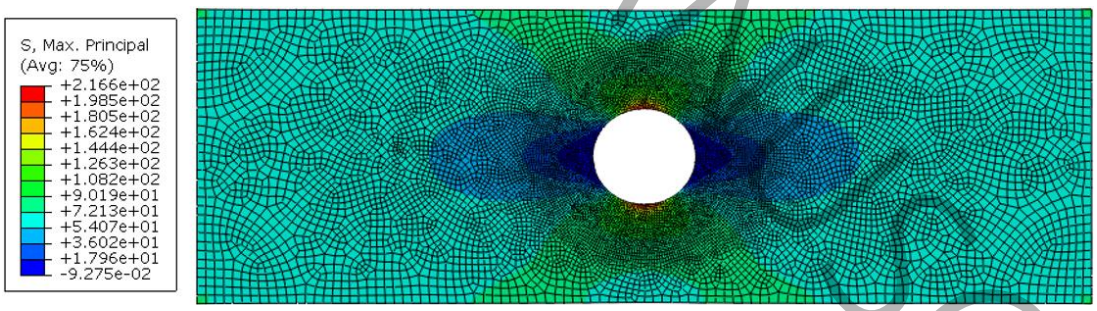

Figure 8-The stress field in the simulation of the macro model for the part with a 10 diameter hole (stress in MPa)

4-2-2- Localization

To investigate the stress field in the micro-scale, or localization, the macro-scale model of the woven composite fabric is made and the analysis is performed according to the characteristics of the homogenized orthotropic material calculated in the homogenization and the applied forces and boundary conditions. Then, the center of the RVE is placed at the location of the desired point for macro-scale localization, and the elements that do not match the geometry of the macro model are removed from the RVE model by an Abaqus script. The boundary conditions calculated in the macro model analysis are applied to the RVE. By implementing the new model, the stress field on the micro-scale in the defined position is determined. As it was mentioned, due to the uncertainties caused by the change in the position of the warp and weft to the hole, it is necessary to repeat these calculations in different situations. In this way, the stress field can

be statistically obtained in different situations. Every position of warp and weft in relation to the hole has a similar chance to accrue. Therefore the statistical models have been produced uniformly.

In Figure 9, the stress field around the hole is shown for some different placement of the warp and weft around the hole. The location of the middle point of the RVE relative to the hole is chosen in such a way that it does not include repeated situations and can cover possible changes in the position of the warp and weft relative to the hole. As can be seen, the position of the maximum stress point and of course its value is different in different situations.

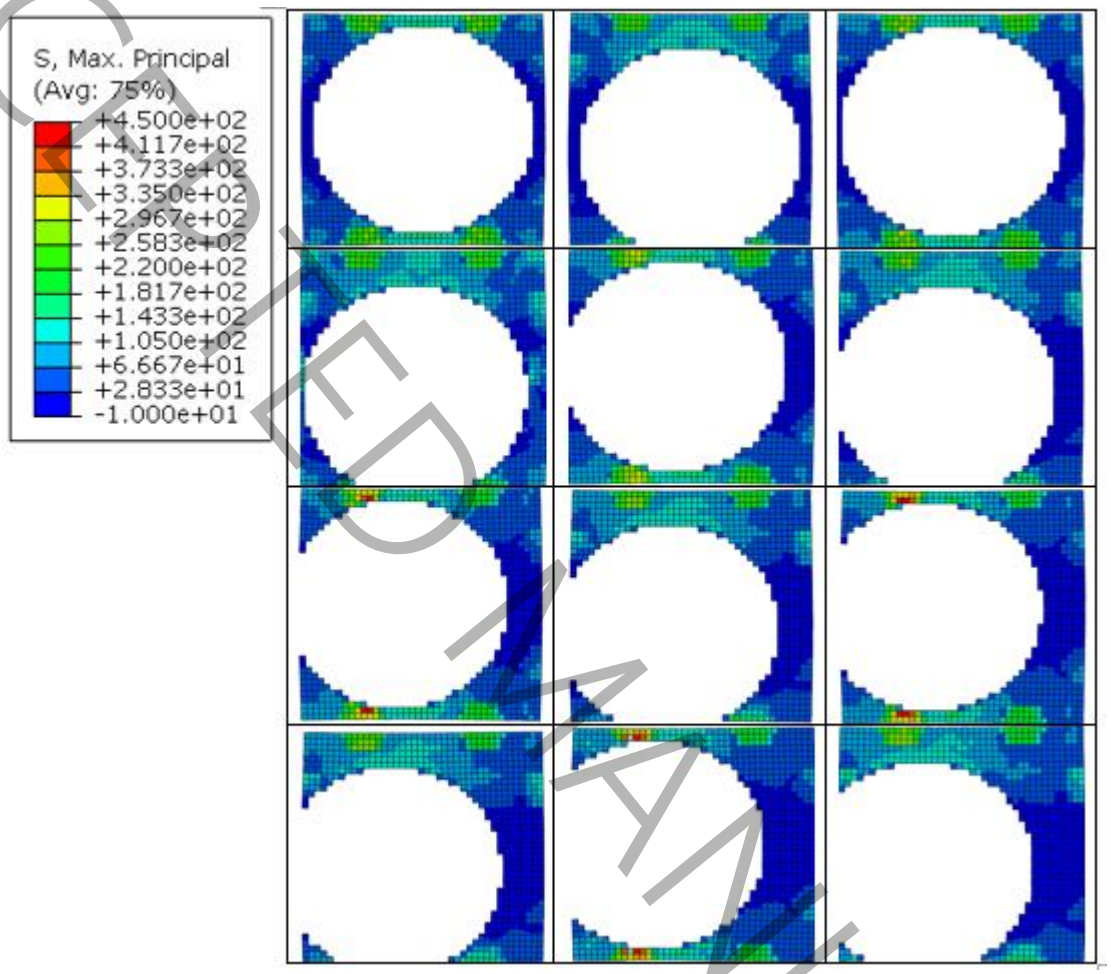

Figure 9- Some of the various localization around the hole in the fabric with a hole of 10 millimeter diameter (stress in MPa)

4-3- Experiment and simulation results

4-3-1- Verification

In this article, for verification, the simulation results have been validated by performing experiments and also by comparing them with analytical equations. For this purpose, the model is simulated with the homogenized properties of an orthotropic plate, similar to the dimensions of the woven composite fabric specimens. Figure 10 shows the elastic strain stress diagram of the part with a 10 millimeters diameter hole in experimental and simulation tests. This graph shows the acceptable agreement of simulation results and experiments in the elastic region. The maximum error measured in this graph is about 7%.

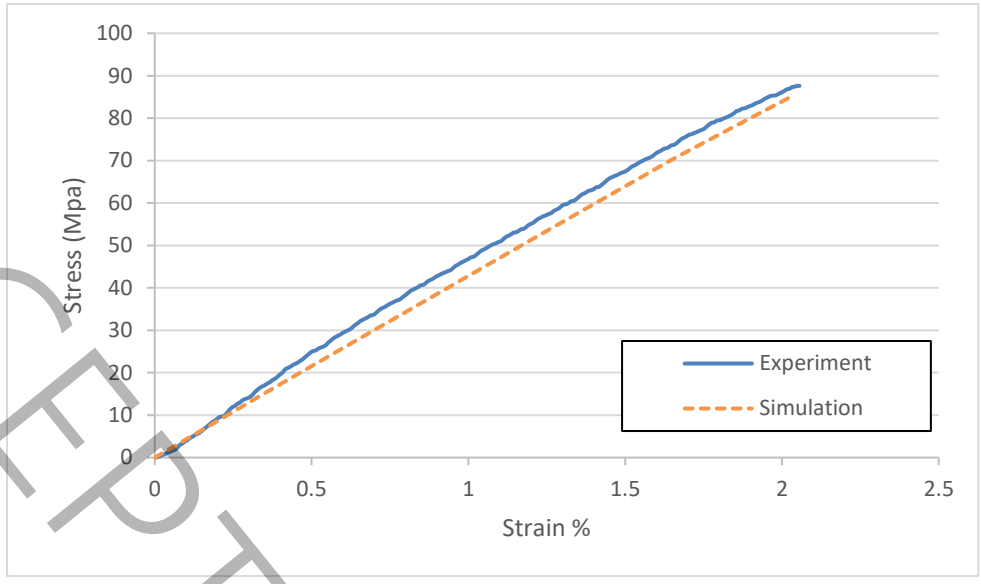

Figure 10-Result comparison of simulation and tensile test in the specimen with a 10 millimeter diameter hole

In terms of the amount of stress increase due to the presence of a hole, comparing the stress simulation results of a homogeneous orthotropic plate under in-plane tensile force in an infinite plate with the stress value calculated from Eq. (1) can show the accuracy of the results. Figure 11 shows this comparison. The horizontal axis of this diagram is the dimensionless distance from the center of the hole in an infinite plate and the vertical axis is the ratio of stress in the tension direction to the average applied stress. This diagram confirms the method used for homogenization and simulation of woven composite fabric.

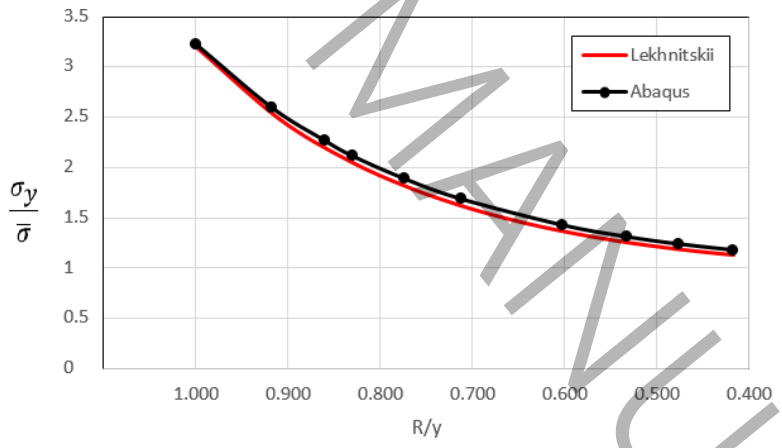

Figure 11-Comparison of the stress ratio in the direction of tension in a fabric with a 10 millimeter diameter hole

4-3-2- Analysis of stress in the microstructure

The uncertainties caused by the position of the yarns around the hole can create different stress fields. Therefore, the amount and location of the maximum stress in the matrix are different. In Figure 12, some stress fields are shown comparatively in different positions of the yarns to the hole.

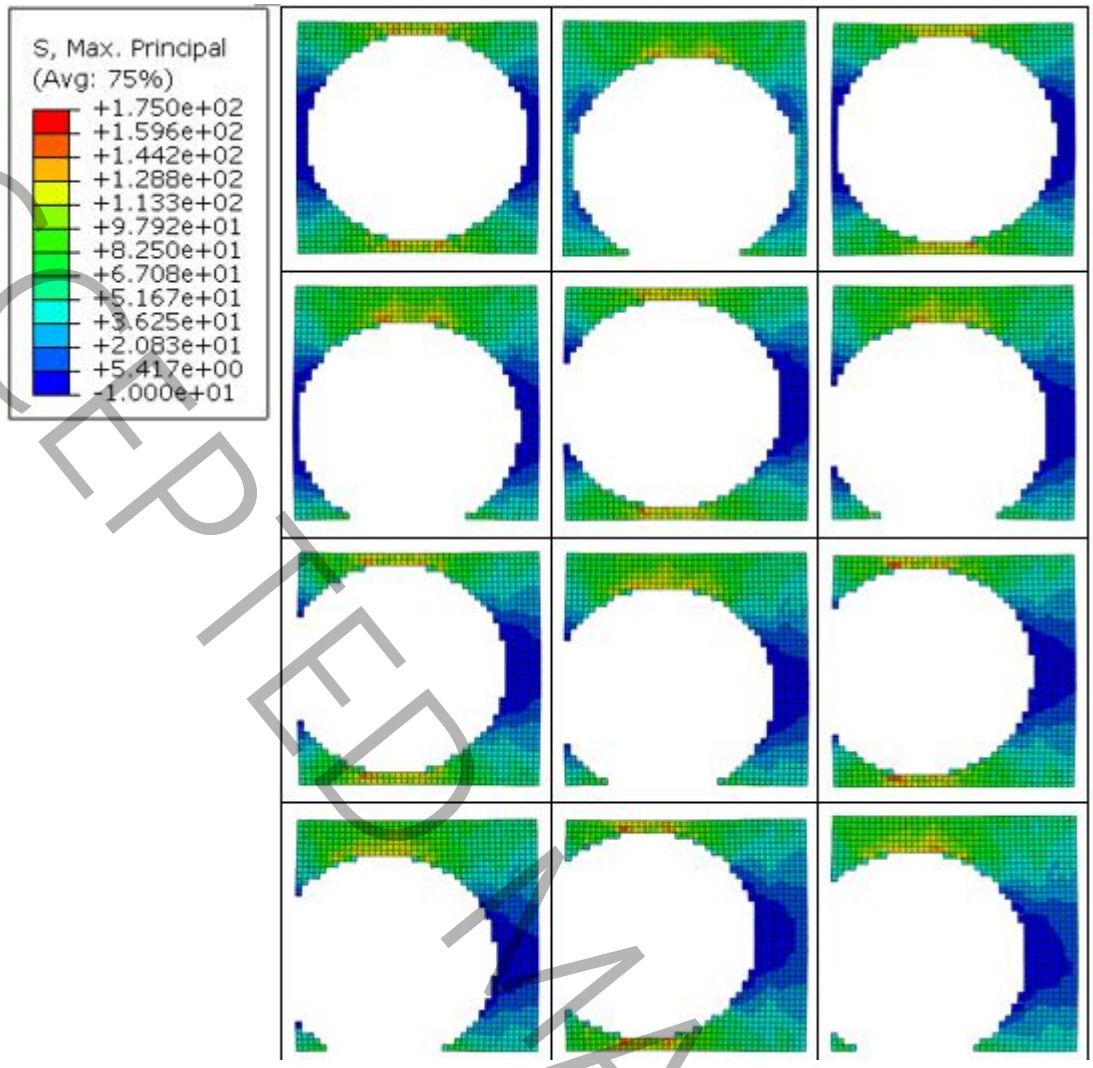

Figure 12-The stress field in the matrix in different positions of the yarns relative to the hole, Stress in MPa (In this figure, only the elements of the matrix are shown and the elements of the yarns are not shown.)

To statistically compare the results obtained in the localization, the histogram diagram of the maximum matrix stress values in different situations of the yarns to the hole for the different hole diameters is drawn in Figure 13. This diagram shows the number and amount of maximum stress around the hole with different diameters at the same strain. It can be seen that with the increase in the diameter of the hole, the average value of the stress around the hole increases.

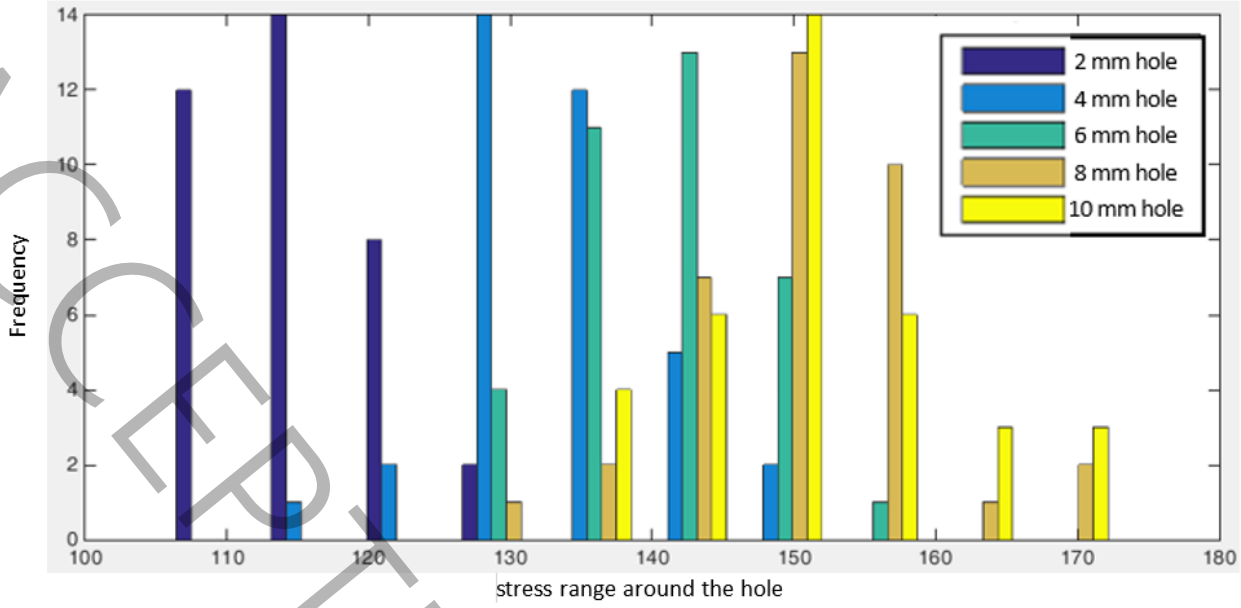

Figure 13-Histogram of stress values in matrix around holes with different diameters

The diagram of Figure 13 shows some overlap of the maximum stresses in different situations. In other words, even though the average amount of stress increases with the increase in the diameter of the hole, there is a possibility that specimens with a smaller diameter hole fail earlier than specimens with a larger diameter hole at the same stress, and this issue is related to the position of the warp and weft to the hole. Therefore, it is not possible to make an explicit prediction about the beginning of matrix fracture in woven composite fabrics with holes. Rather, one can only comment on its probability.

Another result obtained from this diagram is the reduction of the hole size effect at higher diameters. As the diameter of the hole increases, up to 8 millimeters, the value of the maximum stress increases. But as the diameter of the hole increases, the rate of increasing the maximum stress decreases. By increasing the diameter from 8 millimeters to 10 millimeters, there is no significant change in the maximum stress values. Therefor the stress concentration factor has been studied only for 10 millimeter diameter hole.

4-3-3- Ultimate strength analysis in microstructure

Regarding fiber failure prediction, considering that the maximum stress occurs in different places based on the position of the yarns around the hole, statistical analysis like Figure 13 cannot be useful. Figure 14 shows the stress field of the warp and weft in different situations.

As can be seen in Fig. 14, similar to what happens in the matrix, the amount and location of the maximum stress in the fibers change with the change in the position of the warp and weft relative to the hole. Based on this, it is impossible to make an explicit assessment of the ultimate tension of the fibers, and there are uncertainties in this regard.

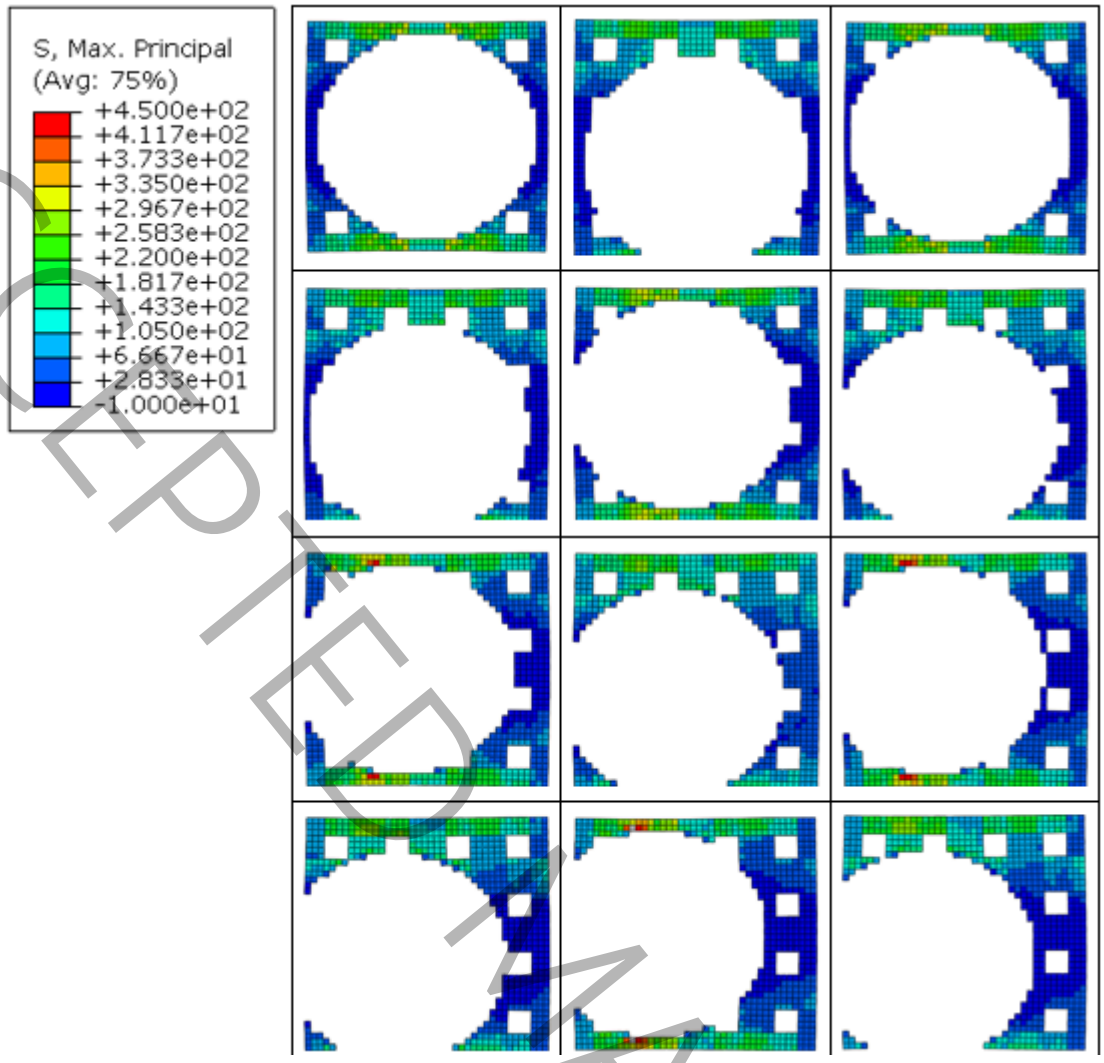

Figure 14-The stress field of warp and weft in different situations (stress in MPa)

4-3-4- Investigating the stress concentration coefficients

By using multi-scale analysis, it is possible to investigate the stress concentration coefficient of woven composite fabric with the hole. For this purpose, the stress fields is studied separately in the matrix and yarns of woven composite fabric with a hole of 10 millimeters in diameter.

Using Chamis criteria for failure of composite materials and considering the stress in regions far from the hole, stress concentration coefficient values can be calculated in different criteria. Due to the probability of different positions of yarns relative to the hole, different analyses were performed in different situations to calculate the values of the stress concentration coefficient range. The minimum and maximum values of stress concentration coefficients are presented in Table 6 for matrix and fiber longitudinal tension. These two criteria have been selected as the primary criteria for composite fiber failure.

Table 6-Minimum and maximum value of coefficients of stress concentration in different criteria

Criteria	Matrix failure in tension	fiber failure in longitudinal tension
Min	2.44	1.97
Max	2.80	3.09

It can be seen that these values have a wide range so it can be concluded that the failure stress value will be variable in different positions of yarns relative to the hole. It is also observed that these two criteria have an overlap and due to this uncertainty, it is impossible to predict the cause of composite failure accurately. The histogram diagram of stress concentration coefficients is shown in Figure 15

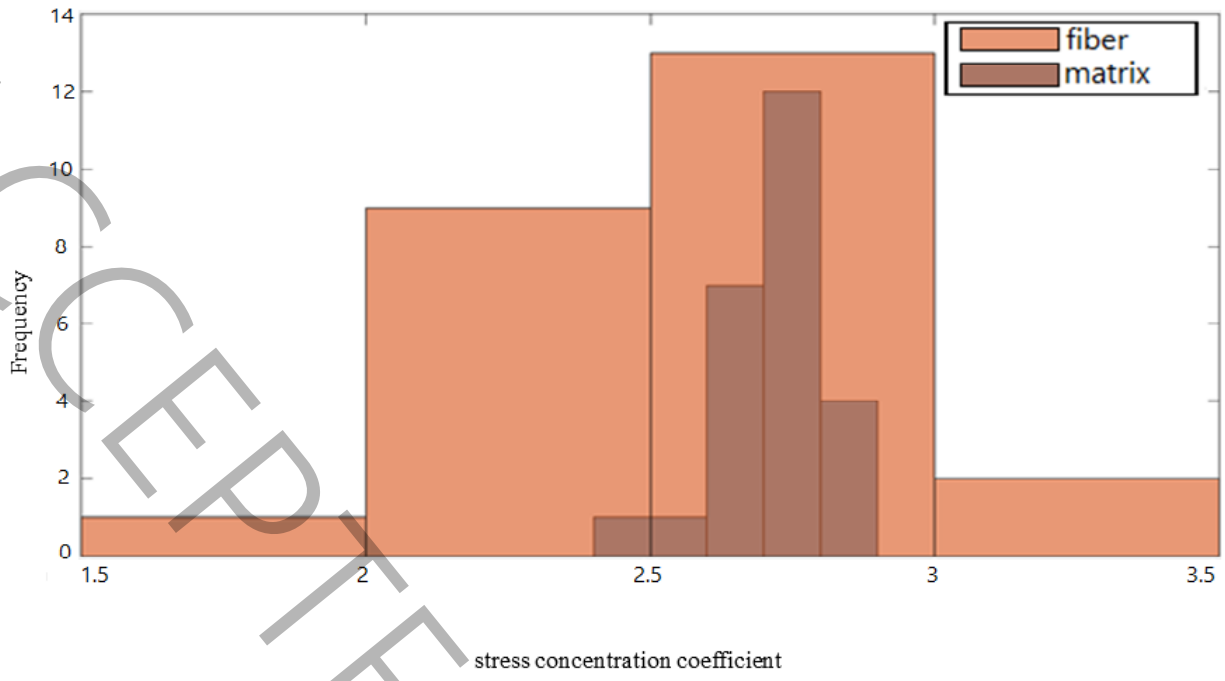

Figure 15-Histogram diagram of stress concentration coefficient for fiber and matrix

From Figure 15, two results can be inferred. The first concerns the initiation of failure, and the second concerns its continuation. It can be seen that despite the spread of the stress concentration coefficient, the highest probability of its occurrence in the fiber is between 2 and 3, and in the matrix between 2.6 and 2.9. The uncertainty in the stress concentration coefficient was less in the matrix than in the fiber. When the overall strength of the matrix is lower, which is generally the case, failure initiates from the matrix, and when the matrix is broken, the fibers provide the overall strength of the material. In this situation, even though no analysis has been performed, it seems that owing to the greater uncertainty in the fiber stress concentration factor, the continuation of the failure process will be completely different from one case to another.

5- Conclusion

Using a multi-scale analysis and evaluation of its results, the effect of a hole in a woven composite fabric was investigated. Homogenization of woven composite from micro to meso scale and from meso to macro scale was done using analytical relations and finite element simulation of the representative volume element, and the results of this homogenization are in good agreement with the experiments and analytical equations. Among the investigated methods for assigning material in finite element simulation in meso scale analysis, it was shown that the method of assigning element by element, which was used in this study, has less error than the embedded method. As a special case, in the example investigated, the energy stored in the embedded method was obtained with a 9% error. Using the displacement results of the simulated homogenized model, localization was performed with the help of a representative volume element around the hole. The study of the maximum stress around the hole shows that in the examined woven composite, the uncertainty caused by the position of the warp and weft to the hole can lead to different values of the maximum stress in the matrix and warp and weft. It was shown experimentally and numerically that the stress around the hole is highly dependent on its dimensions and the amount of stress concentration around the hole is not a certain value. The stress histogram remained stable from the 8 mm diameter hole onwards, and in the 10 mm diameter hole, the highest probability of stress concentration was 2.7. With the multi-scale method used based on the statistical point of view, it is possible to predict the stress concentration coefficient around the hole. In general, with the increase in the diameter of the hole, the value of the maximum average stress increases but the increase in maximum stress is not proportional to the increase in hole diameter. In this way, regarding the part simulated in this article, no significant difference was observed in the value of failure stress in samples with 8 and 10 millimeters

diameter holes. Another result that the simulation at the local scale showed is that due to the existing geometric uncertainties, there is a probability that the specimens with a smaller diameter hole will fail at a lower force than the specimens with a hole with a larger diameter.

Using the multi-scale method, it is possible to predict the stress concentration coefficient around the hole from a statistical point of view. The results show that the stress concentration coefficient values in different criteria for a woven composite fabric can be in a wide range. Consequently, it is not accurate to determine the explicit value of the stress concentration coefficient due to the geometrical uncertainties.

References:

[1] S.A. Kumar, R. Rajesh, S. Pugazhendhi, A review of stress concentration studies on fibre composite panels with holes/cutouts, Proceedings of the Institution of Mechanical Engineers, Part L: Journal of Materials: Design and Applications, 234(11) (2020) 1461–1472.
[2] J.M. Whitney, R.J. Nuismer, Stress Fracture Criteria for Laminated Composites Containing Stress Concentrations, Journal of Composite Materials, 8(3) (1974) 253–265.
[3] J.-K. Kim, D.-S. Kim, N. Takeda, Notched Strength and Fracture Criterion in Fabric Composite Plates Containing a Circular Hole, Journal of Composite Materials, 29(7) (1995) 982–998.
[4] K.N. Surya D. Pandita, Ignaas Verpoest, Strain concentrations in woven fabric composites with holes, Composite Structures, 59 (2003) 361–368.
[5] L. Toubal, M. Karama, B. Lorrain, Stress concentration in a circular hole in composite plate, Composite Structures, 68(1) (2005) 31–36.
[6] J. Li, X.B. Zhang, A criterion study for non-singular stress concentrations in brittle or quasi-brittle materials, Engineering Fracture Mechanics, 73(4) (2006) 505–523.
[7] P.P. Camanho, P. Maimí, C.G. Dávila, Prediction of size effects in notched laminates using continuum damage mechanics, Composites Science and Technology, 67(13) (2007) 2715–2727.
[8] E. Martin, D. Leguillon, N. Carrère, A coupled strength and toughness criterion for the prediction of the open hole tensile strength of a composite plate, International Journal of Solids and Structures, 49(26) (2012) 3915–3922.
[9] B.G. Green, M.R. Wisnom, S.R. Hallett, An experimental investigation into the tensile strength scaling of notched composites, Composites Part A: Applied Science and Manufacturing, 38(3) (2007) 867–878.
[10] P.P. Camanho, G.H. Erçin, G. Catalanotti, S. Mahdi, P. Linde, A finite fracture mechanics model for the prediction of the open-hole strength of composite laminates, Composites Part A: Applied Science and Manufacturing, 43(8) (2012) 1219–1225.
[11] G. Catalanotti, P.P. Camanho, A semi-analytical method to predict net-tension failure of mechanically fastened joints in composite laminates, Composites Science and Technology, 76(4) (2013) 69–76.
[12] A. Arteiro, G. Catalanotti, J. Xavier, P.P. Camanho, Notched response of non-crimp fabric thin-ply laminates: Analysis methods, Composites Science and Technology, 88(2) (2013) 165–171.
[13] J. Modniks, E. Spārniņš, J. Andersons, W. Becker, Analysis of the effect of a stress raiser on the strength of a UD flax/epoxy composite in off-axis tension, Journal of Composite Materials, 49(9) (2015) 1071–1080.
[14] P. Weißgraeber, J. Felger, D. Geipel, W. Becker, Cracks at elliptical holes: Stress intensity factor and Finite Fracture Mechanics solution, European Journal of Mechanics - A/Solids, 55(1) (2016) 192–198.
[15] F.T. Ibáñez-Gutiérrez, S. Cicero, Fracture assessment of notched short glass fibre reinforced polyamide 6: An approach from failure assessment diagrams and the theory of critical distances, Composites Part B: Engineering, 111(10) (2017) 124–133.
[16] D. Taylor, The Theory of Critical Distances: A link to micromechanisms, Theoretical and Applied Fracture Mechanics, 90 (2017) 228–233.
[17] M.M. Moure, J. Herrero-Cuenca, S.K. García-Castillo, E. Barbero, Design tool to predict the open-hole failure strength of composite laminates subjected to in-plane loads, Composite Structures, 238 (2020) 111970.

[18] A. Dixit, H.S. Mali, MODELING TECHNIQUES FOR PREDICTING THE MECHANICAL PROPERTIES OF WOVEN-FABRIC TEXTILE COMPOSITES A REVIEW, Mechanics of Composite Materials, 49 (2013) 1–20.
[19] J.J. Crookston, A.C. Long, I.A. Jones, A summary review of mechanical properties prediction methods for textile reinforced polymer composites, Proceedings of the Institution of Mechanical Engineers, Part L: Journal of Materials: Design and Applications, 219(2) (2005) 91–109.
[20] P. Tan, L. Tong, G.P. Steven, Modelling for predicting the mechanical properties of textile composites—A review, Composites Part A: Applied Science and Manufacturing, 28(11) (1997) 903–922.
[21] A. Tabiei, Y. Jiang, Woven fabric composite material model with material nonlinearity for nonlinear finite element simulation, International Journal of Solids and Structures, 36 (1999) 2757-2751.
[22] P. Rupnowski, M. Kumosa, Meso- and micro-stress analyses in an 8HS graphite/polyimide woven composite subjected to biaxial in-plane loads at room temperature, Composites Science and Technology, 63(6) (2003) 785–799.
[23] S. Kim, C. Lee, H. Shin, L. Tong, Virtual experimental characterization of 3D orthogonal woven composite materials, in: 19th AIAA Applied Aerodynamics Conference, 2013, pp. 1570.
[24] H. Lin, M.J. Clifford, A.C. Long, K. Lee, N. Guo, A finite element approach to the modelling of fabric mechanics and its application to virtual fabric design and testing, Journal of the Textile Institute, 103(10) (2012) 1063–1076.
[25] Woven Composites, Imperial College Press, 2015.
[26] S.A. Tabatabaei, S.V. Lomov, I. Verpoest, Assessment of embedded element technique in meso-FE modelling of fibre reinforced composites, Composite Structures, 107 (2014) 436–446.
[27] C. Fagiano, E. Baranger, P. Ladeveze, M. Genet, Computational strategy for the mesoscale modeling of thermostructural woven composites, ECCM 2012 - Composites at Venice, Proceedings of the 15th European Conference on Composite Materials, (2012).
[28] N.-Z. Chen, C. Guedes Soares, Spectral stochastic finite element analysis for laminated composite plates, Computer Methods in Applied Mechanics and Engineering, 197(51-52) (2008) 4830–4839.
[29] J.R.M. Fazilat H. Dar, Richard M. Aspden, Statistical methods in finite element analysis, Journal of Biomechanics, 35 (2002) 1155–1161.
[30] G. Stefanou, D. Savvas, M. Papadrakakis, Stochastic finite element analysis of composite structures based on material microstructure, Composite Structures, 132(9) (2015) 384–392.
[31] M. Ibrahim, effect of notch size on reliability of composit laminates based on SFEM and experimental investigation, Concordia University, 2005.
[32] L. S.G., Anisotropic Plates, Gordon and Breach Science Publishers, 1984.
[33] S.D. Pandita, K. Nishiyabu, I. Verpoest, Strain concentrations in woven fabric composites with holes, Composite Structures, 59(3) (2003) 361–368.
[34] C.C. Chamis, Simplified composite micromechanics equations for strength, fracture toughness and environmental effects, SAMPE Quarterly, 15 (1984).
[35] J. Aboudi, S.M. Arnold, B.A. Bednarcyk, Micromechanics of Composite Materials: A Generalized Multiscale Analysis Approach, in, Elsevier, 2013.
[36] R. Hill, Elastic properties of reinforced solids: some theoretical principles, J. Mech. Phys. Solids, 11 (1963) 357–372.
[37] R. Younes, A. Hallal, F. Fardoun, F. Hajj, Comparative Review Study on Elastic Properties Modeling for Unidirectional Composite Materials, in: N. Hu (Ed.) Composites and Their Properties, InTech, 2012.
[38] C. C.C., Mechanics of Composite Materials Past, Present and Future, Journal of Composites Technology and Research, (11) (1989) 3–14.
[39] C.T. Herakovich, Mechanics of fibrous composites, John Wiley and Sons, Inc, 1998.
[40] A. Kemp, An Extension of Peirce's Cloth Geometry to the Treatment of Non-circular Threads, Journal of the Textile Institute Transactions, 49(1) (1958) T44-T48.